Geopersia ***6*** *(2), 2016, PP. 265-282*

Karstification Potential Mapping in Northeast of Khuzestan Province, Iran, using Fuzzy Logic and Analytical Hierarchy Process (AHP) techniques

Samad Moradi *, Nasrollah Kalantari, Abbas Charchi
Department of Geology, Faculty of Earth Sciences, Shahid Chamran University, Ahvaz, Iran
**Corresponding author, e-mail: samadmoradi39@yahoo.com*
(*received: 11/02/2016 ; accepted: 25/09/2016*)

Abstract

The primary objective of the current study is to produce karstification potentiality maps in northeast of Khuzestan province, Iran, using both fuzzy logic and AHP models as an additional tool in hydrogeological research. Geographic Information Systems (GIS) and Remote Sensing (RS) are used to create two maps depicting the development of the karstification, consisting of five classes, showing the karstification potentiality ranging from very high to very low. The extractions of these maps are based on the study of input data such as: lithology, lineament density, elevation, slope, rainfall, temperature, drainage density and vegetation cover. Eventually, two maps based on weighted spatial modeling system are created. The verification results show that the fuzzy logic model outperformed AHP model for the study area. Based on hydrogeological survey, hydrodynamic characteristics perceived at the outlet of major springs consisting of Dare-Anari (DA), Abshekaloo (AS) and Sarhooni (SH) revealed poorly and well developed karstified systems. The collected data indicated that one of the main factors for karst development in the area is tectonic activity and occurrence of lineaments in various scales.

Keywords: *Karstification Potential, GIS, Remote Sensing, AHP, Fuzzy Logic.*

Introduction

Karstified carbonate formations are among the most important water resources in the southern and western regions of Iran (Karimi *et al.*, 2003; Ashjari & Raeisi, 2006). Karstification typically occurs in biogenic, biochemical and chemical sedimentary rocks; mostly in carbonate rocks such as limestone and dolomite (Johnson & Stieglitz, 1990; Groves & Meiman, 2005; De Waele *et al.*, 2009) and also in sulphate rocks such as gypsum and anhydrite (Black, 1997; Calaforra & Pulido-Bosch, 2003). Characteristic karst landforms include solutionally-enlarged factures and channels (karren) as well as closed depressions of differing origins, structure and dimensions (dolines, poljes). Cvijic (1893) described dolines as "the diagnostic karst landforms" (Ford, 2007). Karst landscapes are characterized by fluted and pitted rock surfaces, shafts, sinkholes, sinking streams, springs, subsurface drainage systems and caves. The unique features and three-dimensional nature of karst landscapes are the result of a complex interplay between geology setting, climate condition, and biological factors over the long time scales. Karst landscapes in which dissolution of bedrock by water is the dominant geomorphic process, characterize almost 20% of the continents and more than a quarter of the Earth's population lives on or near karst areas (Ford & Williams, 2007). Karstification has many practical implications: Sinkholes in karst areas are geotechnical hazards for houses, streets and other infrastructure (Field, 2010; Vigna *et al.*, 2010); Reservoirs and other hydraulic infrastructure in karst often exhibit leakage problems (Bonacci & Roje-Bonacci, 2008; Bonacci *et al.*, 2009a); Karst areas exhibit significant biodiversity at the surface, underground and in groundwater-dependent ecosystems (Humphreys, 2006; Bonacci *et al.*, 2009b); Karst aquifers are valuable freshwater resources but highly vulnerable to contamination as they consequently require special protection (Ravbar & Goldscheider, 2007). Deep karst aquifers are valuable geothermal resources (Goldscheider *et al.*, 2010).

Carbonate karstic formations outcrop in about 23% of the Zagros Region (Ashjari & Raeisi, 2006). The age of these karst formations is related to Cenozoic era. Karst in Zagros zone as compared to such formations in other regions of Iran has differences, owing to the regularity of folding in Zagros and being comprised of carbonate and non-volcanic rocks, so that carbonate rocks makes 95% of the mountains (Maleki *et al.*, 2009). Carbonate rocks in Zagros are affected by tectonic insertion factors and cold climate with long rainfalls which have caused the maturation and the evolution of karst and have made so many caves such as "Ali Sadr" and "Shapour" (Moghimi, 2010). Fractures

made in carbonate rocks due to tectonic factors are a sequential phenomenon in the Zagros Mountains Chain and substantially it is the first stage of karstification (Maleki *et al.,* 2009). Desert land encompasses two thirds of Iran's landmass which is devoid of forests and green pastures. Such a harsh environmental condition and water scarcity have led Iranian people to mostly rely on groundwater resources than surface water (Baghvand *et al.,* 2010; Bastani *et al.,* 2010; Nosrati & Eeckhaut, 2012). On the other hand, having knowledge on karstic water resources and potential mapping always requires sophisticated costly instruments and methodology as well. Remote Sensing (RS) and Geographic Information Systems (GIS) are proved as useful tools in karstification potential mapping. Antonakos *et al.* (2014) applied multicriteria analysis within GIS environment in order to produce a distribution map of site suitability for drilling new production boreholes in Korinthia Prefecture (Greece). Konkul *et al.* (2014) applied a similar method to map the hydrogeological characteristics and groundwater potentiality of Huay Sai area (Thailand) using potential surface analysis. Chitsazan *et al*. (2015) compared karst development in two main zones Keyno anticline (Zagros Range) and Shotori anticline (Central Iran) of Iran. They used isotopic, hydrochemical and geomorphological data and they concluded arid karst aquifers have different characteristics compared with, typical karst aquifers. Fu Yeh *et al.* (2016) presented the estimation of groundwater recharge using GIS approach and integrated five contributing factors: lithology, land cover/land use, lineaments, drainage, and slope can be pointed out.

In Iran, more than 70 % of the rural and nearly 50% of the urban populations depend on groundwater resources for meeting their drinking and domestic requirements (Rahmati, 2013). Unfortunately, water scarcity is common in several parts of Iran that is being exacerbated by human activities and global climate change (Ghayoumian *et al.,* 2007; Abbaspour *et al.,* 2009; Ayazi *et al.,* 2010; Zarghami *et al.,* 2011; Hosseini *et al.,* 2012; Neshat *et al.,* 2013). It seems that such conditions are to some extent similar around the arid and semi-arid areas of the world.

This paper presents the study of karstification potentiality map ping of the wide area of northeast of Khuzestan province area (southwest Iran) with the contribution of Remote Sensing and Geographic Information System, which aims to establish a supple mentary or amending tool in locating karstic developed area. For this reason, rainfall data, hydrogeological, geomorphological and geological data as well as both AHP and Fuzzy logic methods are used for preparing karstification potentiality finals maps. Furthermore, the reliability of karstification potentiality mapping is controlled by using hydrogeological and geomorphological data. Assessing the karstification potential will be helpful for decision makers in karstic water resources management and identifying suitable locations for drilling production wells.

Physical setting of the area

The study area is located in southwest Iran, in the region of Khuzestan, occupying an area of 4314 km^2 (Fig. 1). The geomorphological development of the region is characterized by mild to relatively high relief with altitudes ranging from 314m to 3741m. Climatologically, the study area falls in semi-arid to semi-humid temperate climatic condition with cold winters and moderate summers. The monthly minimum temperature average is 9.8°C in the January and monthly maximum temperature average is 32.1°C in the August. In the last 30 years, the mean annual rainfall has been 780 mm and the most rainfall occurs from November to the end of April. Karun River and Taloog River which gathers almost all the runoff of the study area and have a total length of 60 km and 30 km respectively, dominates in the drainage network of the wider region.

Concerning its' lithology, it is subsumed in the folding Zagros zone and consists of alluvial deposits, shale, marl, siltstone, gypsum, sandstone, conglomerate, dolomite and limestone formations (Fig. 1). The geological bedrock consists of shale and marl which are almost impermeable. Limestones and dolomites are 200-400m thick and their permeability factor due to the existence of intense karst phenomena and tectonics is high. The main aquifers are developed within limestones and dolomites and they cover major parts of the study area.

Geological setting

The geological settings is very important, especially the nature of the overlying and underlying units and the topography. From the geological point of view, the basin is located in the Zagros Fold Belt, which has a main NW-SE trend. The outcrops of the region are the sequence of the Zagros Mountains Chain and have an age equal to Alpine folding. The

outcrop layers in the studied zone are comprised of geosynclines sediments of Zagros zone and the age of which is from the early Cretaceous to the present era. The outcrops are the result of Alpine orogeny; started from the late Triassic and continued to the end of Pliocene (Aghanabati, 2004). The geological formations in the region from old to new are shown in table 1.

Table 1. The geological formations and its description in the study area

Formation name	Lithology	Age	%Area in the region
Daryan	Limestone	Aptian-Albian	0.5
Garau	Shale	Neocomian-Coniacian	4
kazhdomi	Shale	Albian- Cenomanian	0.7
Ilam-Sarvak	Limestone	Albian-Santonian	34
Gurpi	Marl and Shale	Santonian- Maastrichtian	8
Tarbur	Limestone	Companian-Masstrichtian	1
Amiran	Sandstone, Siltstone, Conglomerate	Paleocene	1
Pabdeh	Marl and Shale	Paleocene	5
Talezang	Limestone	Paleocene- Eocene	2
Kashkan	Conglomerate, Sandstone, Siltstone	Eocene	1.1
Shahbazan	Limestone	Eocene	0.3
Asmari	Limestone and Dolomite	Paleocene-Miocene	24
Gachsaran	Marl, Gypsum/Anhydrite and Halite	early Miocene	1
Razak	Marl	early Miocene	0.3
Mishan	Marl and Shale	early-middle Miocene	0.8
Aghajari	Sandstone and Siltstone	Miocene- late Pliocene	2
lahbari	Marl and Siltstone	Pliocene	0.3
Bakhteyari	Conglomerate	Pliocene	2
Recent alluvium	Alluvium	Pleistocene- Holocene	12

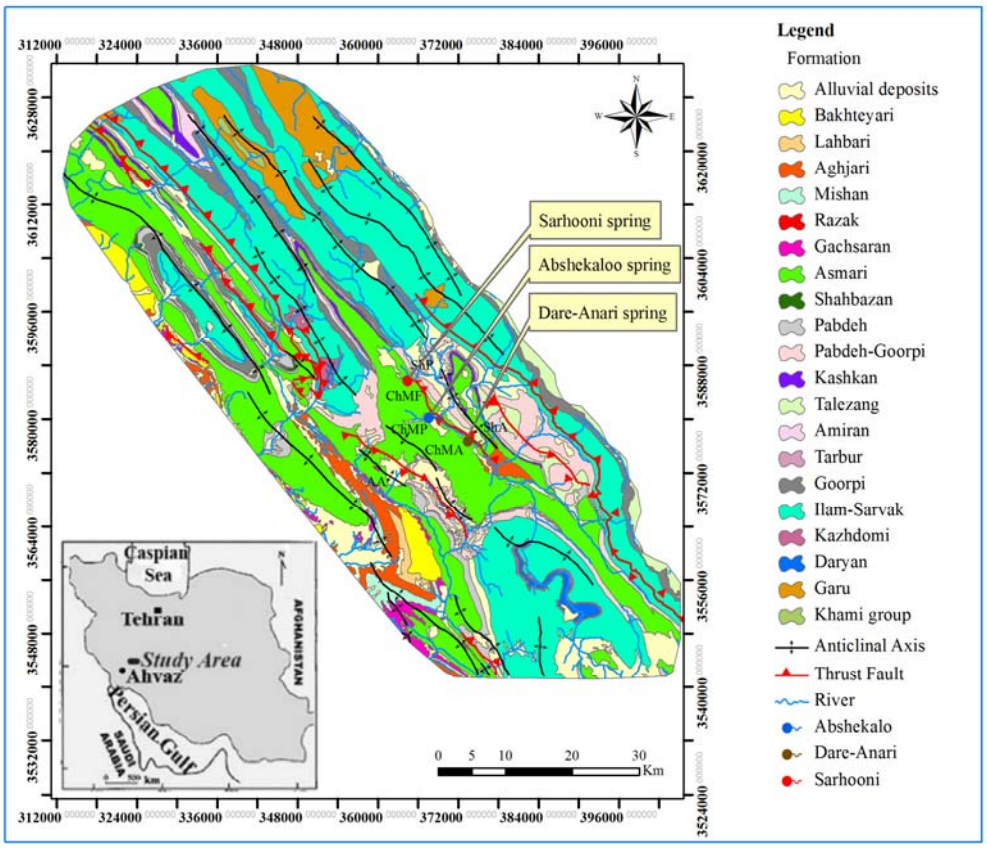

Figure 1. Location and geology map of the study area.

The detailed lithology of these formations has been described by James and Wynd, (1965); Stocklin and Setudehnia, (1977); and Alavi, (2004). The area is dominantly covered by Asmari carbonate Formation and the Asmari karstic litho-units overlie the inherently impermeable Pabdeh-Gorpi units where the latter acts as a hydraulic barrier.

Tectonics and Structural Geology

The study zone is considered as part of Zagros folded region, which has a simple and gentle geological structure including sequences of close anticlines with usually vertical axial plane. The mountainous study area is characterized by intensive tectonic processes resulted in developed structural features such as anticlines, faults and fractures. Lithology and tectonic activities are the most important determinant of karst development occurrence in the study area. Structural features like Shelar anticline (ShA), Chaleh-Monar anticline (ChMA) and Aram anticline (AA), Chaleh- Monar thrust fault (ChMF) trending NW-SE, parallel to the general structure of Zagros structural belt and Chale-Monar polje (ChMP) and Shelar polje (ShP) are outstanding geomorphological features in the study area (Fig. 1). ChMF is one of the important faults, which have caused ChMP. This thrust in the east region and with a length of about 16 kilometers; causes uplift ShA on the ChMA. In addition, the presence of DA karst spring with an average discharge of $4m^3/s$ and the formation of other springs such as SH and AS in the region are the result of the thrust function possibly. There are two major faults in both eastern and western parts of the study area and other minor faults, which have shaped the ChMP and the ShP. Different topographic, tectonic and geological evidences of the region indicate the same fact. In general, intensity of lineaments in ChMA is considerable and resulted in the incidence of fracture frequency, intensive karstification and accordingly, facilitates groundwater movement. Geological and geomorphological structures play a key role in groundwater movement and similarly local and regional impact on flow pattern (Kalantari *et al.,* 2011). The impermeable Pabdeh-Gurpi Formation forms the core of the anticlines and groundwater moves on the top of this hydraulic obstruction.

Materials and method

In order to conduct the present study, the following data and software are used: geological maps covering the study area (sheets: Lali, Keyno, Kamestan, 1:100,000 scale, source: Institute of Geology) meteorological and climatological data. Image processing software: ENVI 4.8. GIS software: ArcGIS 9.3. Expert choice 11 are being used.

Geological maps of the study area were scanned, imported into ArcGIS 9.3 and georeferenced to the UTM/WGS84 projection system. Using ENVI 4.8 software, the bands of the satellite image were initially ‘‘layer stacked’’, and georeferenced, then the file was resized so that only the broader study area was included, then it was radiometrically corrected (log-residuals option) and finally a proper false color composite image was created. Then, creation of thematic maps took place, using lithology, lineament density, elevation, slope, rainfall, temperature, drainage density, and vegetation cover. A weighted spatial probability modeling was applied to identify karstification potential areas, according to their relevance to the development of karstification. Eventually, karstification potentiality maps were created, consisting of five gradational poten tiality classes, ranging from very low to very high (Figures 4 & 6). The mathematical methods of Analytical Hierarchy Process (AHP) and Fuzzy logic, which were introduced by Saaty (1980) and Lotfizade (1965) respectively, were used to derive the final karstification potentiality maps. It should be noted that AHP method has been applied in many hydrogeological studies for site suitability analysis (Banai-Kashani, 1989; Pourghasemi *et al.*, 2012). To do so, the individual karstification potentiality factors were given values (weights) according to their significance. In order to achieve this, all the factors were paired with each other and following that each factor was given an arithmetic value between 1 and 9, according to their significance when compared to the other factor with which it formed the pair (Table 3).

Then, the karstification potentiality map was produced in accordance with the mathematical equation (1) below:

$$M = w_1x_1 + w_2x_2 + w_3x_3 + w_4x_4 + w_5x_5 + w_6x_6 + w_7x_7 + w_8x_8 \quad (1)$$

Where M is the value for each pixel of the final karstification potentiality map of the study area. Variables w_1, w_2, w_3, w_4, w_5, w_6, w_7 and w_8 are the weight values for each preparatory factor and variables x_1, x_2, x_3, x_4, x_5, x_6, x_7, x_8 are the rating values for each pixel according to the preparatory factor to

which it is referred (Domakinis *et al.*, 2008). The quantitative parameters were classified according to the grading method of equal intervals of ArcGIS 9.3. This method has been used in the classification of hydrogeological studies as well as in the classification of vulnerability degrees (Huan *et al.*, 2012; Kazakis & Voudouris, 2015). The eight factors for karstification potentiality mapping (lithology, lineament density, elevation, slope, rainfall, temperature, drainage density, and vegetation cover) are separately examined in the following paragraphs. The thematic maps portray the eight factors extracted for the calculation of the final maps. The values' range was reclassified based on different classes, with variable intervals (Table 2). The reclassification was performed based on the potentiality of karstification development. The factors' weights used are related to the participation of each factor on the karstification expansion. All maps were classified. The weights were adopted and optimized from the results of experience or judgments of experts in similar previous works on karstification potentiality mapping (Elewa & Qaddah, 2011). The effectiveness (last column of table 2) of each factor parameter is calculated by multiplying its weight by the rate (Al Saud, 2010). Factors with more value of effectiveness have more effects on karstification potentiality. Like the map prepared using the AHP method, the second map of karstification potentiality was prepared using fuzzy logic method and classified, and shown in Figure 6.

Selecting thematic layers influencing karstification potential

The number of used thematic layers depends on the data availability in the study area. In order to assess karstification potential zones, eight thematic layers namely lithology, lineament density, elevation, slope, rainfall, temperature, drainage density and vegetation cover are chosen as the effective factors. Hydrology conditions are largely dependent on these thematic layers and hence influence the occurrence of karstification.

These thematic layers provide a reliable ground for an effective prediction of the karstification potential of a given area. The whole process of the karstification potential prediction is shown in Figure 2.

Table 2. Pairwise comparison matrix, factor weights and consistency ratio of the data Layers

Factors	1	2	3	4	5	6	7	8	9	weights
Lithology										
(1)Shale	1	1	1/9	1/5	1/8	1/4	1	1	1/5	0.026
(2) Alluvium		1	1/9	1/5	1/8	1/3	1	1	1/6	0.026
(3) Limestone			1	5	2	6	9	9	3	0.339
(4) Sandstone				1	1/2	2	4	4	1/3	0.102
(5) Dolomite					1	4	6	6	3	0.225
(6) Siltstone						1	3	3	1/3	0.068
(7) Marl							1	1	1/6	0.028
(8) Gypsum								1	1/6	0.028
(9) Conglomerate									1	0.159
Consistency ratio:0.03										
Slope(°)										
(1)<5	1	3	5	7	9					0.513
(2) 5-10		1	3	5	7					0.261
(3) 10-15			1	3	5					0.129
(4) 15-35				1	3					0.063
(5)>35					1					0.033
Consistency ratio:0.05										

Table 2. Continued

Factors	1	2	3	4	5	6	7	8	9	weights
Drainage density										
(1) <40	1	3	5	7	9					0.513
(2) 40-80		1	3	5	7					0.261
(3) 80-120			1	3	5					0.129
(4) 120-160				1	3					0.063
(5)>160					1					0.033
Consistency ratio:0.05										
Rainfall(mm)										
(1) <750	1	1/3	1/5	1/7	1/9					0.033
(2) 750-900		1	1/3	1/5	1/7					0.063
(3) 900-1050			1	1/3	1/5					0.129
(4) 1050-1200				1	1/3					0.261
(5) >1200					1					0.513
Consistency ratio:0.05										
Vegetation cover										
(1) Dense cover	1	3	5							0.648
(2) Moderate cover		1	2							0.230
(3) Low cover			1							0.122
Consistency ratio:0.01										

Table 2. Continued

Elevation	1	2	3	4	5	6	7	8	9	weights
(1) <987	1	1/3	1/4	1/6	1/7					0.043
(2) 987-1459		1	1/2	1/3	1/6					0.089
(3) 1459-1980			1	1/2	1/4					0.145
(4) 1980-2672				1	1/2					0.255
(5) >2672 m					1					0.469
Consistency ratio:0.02										
Temperature										
(1) <11.7	1	3	5	7	9					0.532
(2) 11.7-15.2		1	2	4	6					0.232
(3) 15.2-17.8			1	2	4					0.127
(4) 17.8-20.2				1	2					0.068
(5) >20.2 °C					1					0.040
Consistency ratio:0.02										
Lineament density										
(1)<49	1	1/3	1/5	1/7	1/9					0.036
(2) 49-113		1	1/2	1/4	1/6					0.080
(3) 113-194			1	1/2	1/4					0.145
(4) 194-331				1	1/2					0.269
(5)331-673					1					0.471
Consistency ratio: 0.02										

Table 3. Matrix of factors' weights evaluation

	(a)	(b)	(c)	(d)	(e)	(f)	(g)	(h)	Weights
Lithology (a)	1	3	4	5	6	7	8	9	0.387
Lineament density (b)		1	2	3	4	5	6	7	0.209
Precipitation (c)			1	2	3	4	5	6	0.144
Elevation (d)				1	2	3	4	5	0.098
Vegetation cover (e)					1	2	3	4	0.066
Temperature (f)						1	2	3	0.044
Drainage density (g)							1	2	0.031
Slope (h)								1	0.022
									CI=0.04

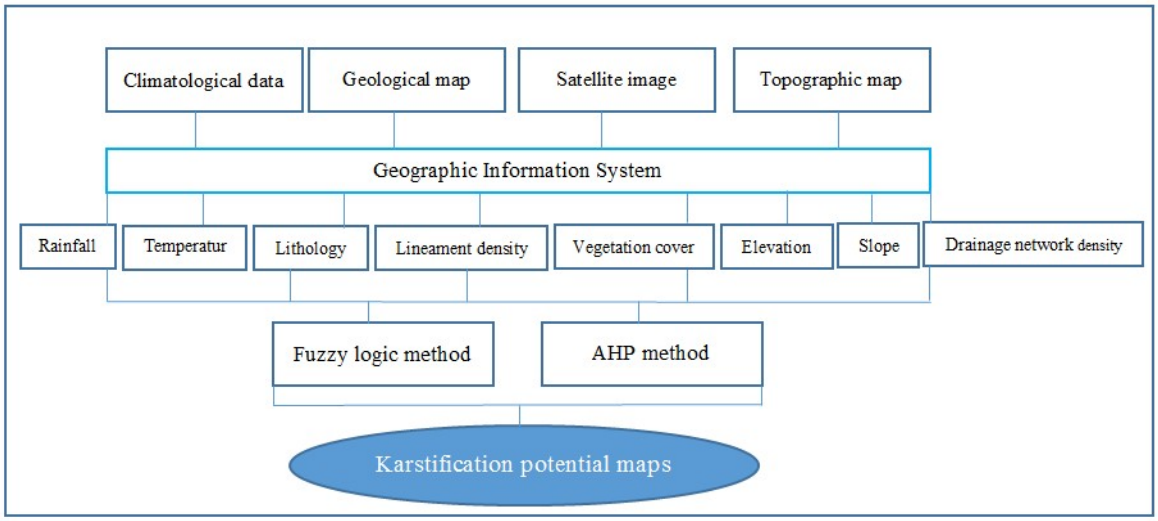

Figure 2. Flow chart of the methodology for assessing the karstification potential of the study area

Factors influencing karstification

Lithology

Lithology factor (weight 38% or 0.38) is associated with water permeability and ability of the formations to host groundwater. Fracture systems, joins, dykes and porosity influence the capacity and specific storage of groundwater among various rock types. Along with primary porosity, sedimentary aquifers have higher capacity and specific storage of groundwater than the karst and fissured rock aquifers in which the groundwater interesting is locally and predominately in faults and fractures. The geological map was derived from the available geological maps with scale 1:100,000 from Institute of Geology and Mineral Exploration. Different rocks were digitized as polygons and thus the thematic map was produced. Consequently, the map of Figure 3a was created and divided into 9 classes. Shale, marl, siltstone and gypsum are impervious geological formations and create a barrier to groundwater infiltration while they have low storage capacity of groundwater. Other formations are including limestone, dolomite, sandstone, conglomerates and recent alluvium.

Lineament density

A lineament is a linear feature in a landscape which is an expression of an underlying geological structure such as a fault. For the extraction of lineaments' density map, a satellite image Landsat-7/ETM^{+} was initially processed in ENVI 4.7, in order to determine the most appropriate False Color Composite/FCC image for lineaments' delineation. Combination of bands 753: RGB (Red/ Green/Blue) was proved to be the most suitable for this purpose. After the lineaments' (satellite image) and faults' (geological map) digitization, their density was calculated in Arc map 9.3 (Line Density command). Next, a reclassification of the raster lineament density file followed into 5 classes, from very low to very high, according to the class boundaries of table 2, yielding Figure 3b map. The lineament density raster file was assigned a weight of 20% (0.20) in the calculation of the karstification

potentiality final map, according to AHP methodology. It should be noted that in the area of gray color, where no faults and lineaments exist, the potentiality of the karstification is low, in contrast with the red colored area, where the probability reaches its maximum level.

Elevation

Elevation is one of the controlling factors in the karstification and was assigned a weight of 9% (0.09) in the final karstification potentiality value. Elevation influences to karstification are often displayed as indirect relationships or by means of other factors. In general, topography plays a key role in the recharge, discharge and emerges of karstic springs. With an increase in height in a region, due to increased hydraulic gradient, karst development potential will be increased.

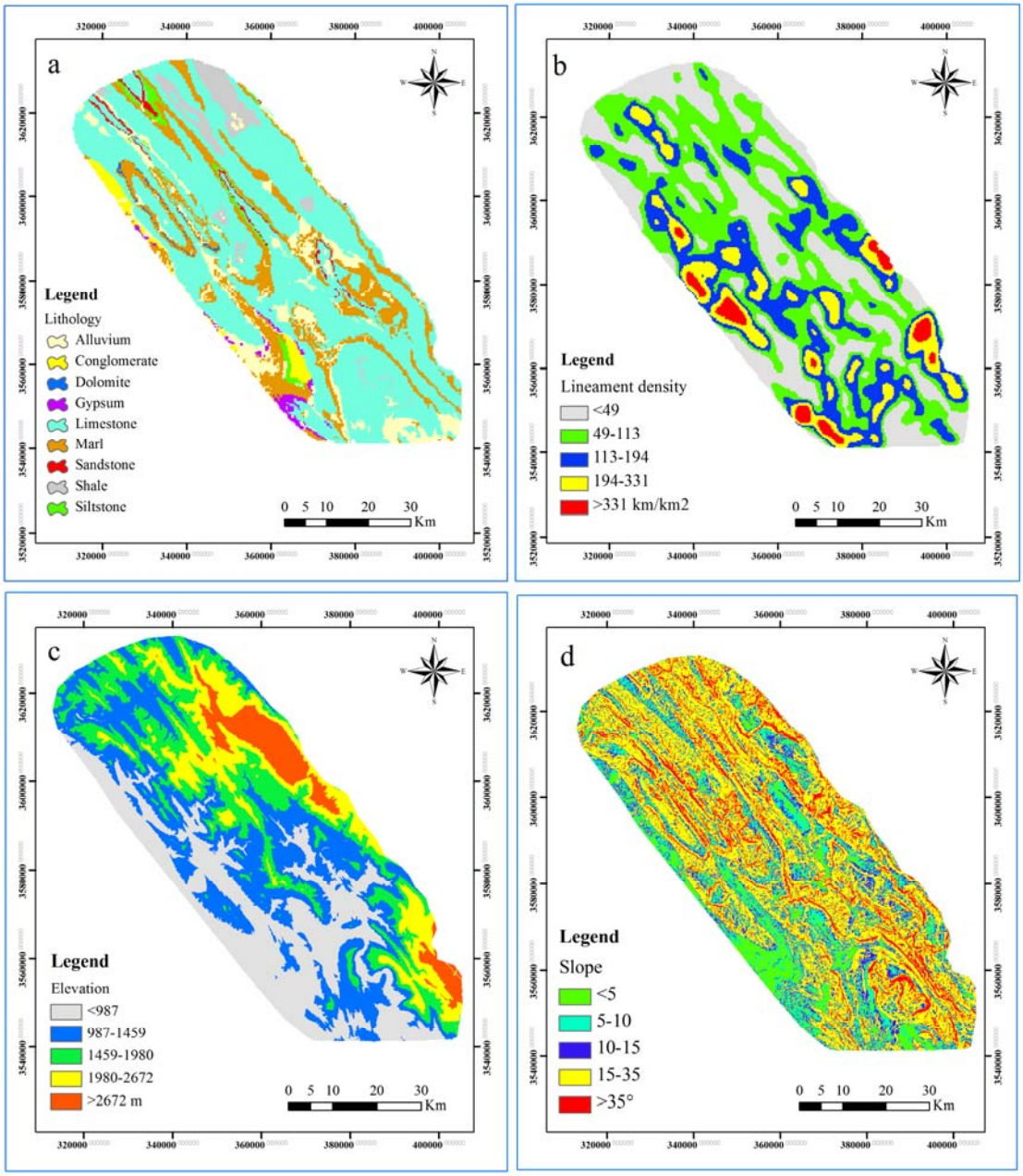

Figure 3. Continued on the next page

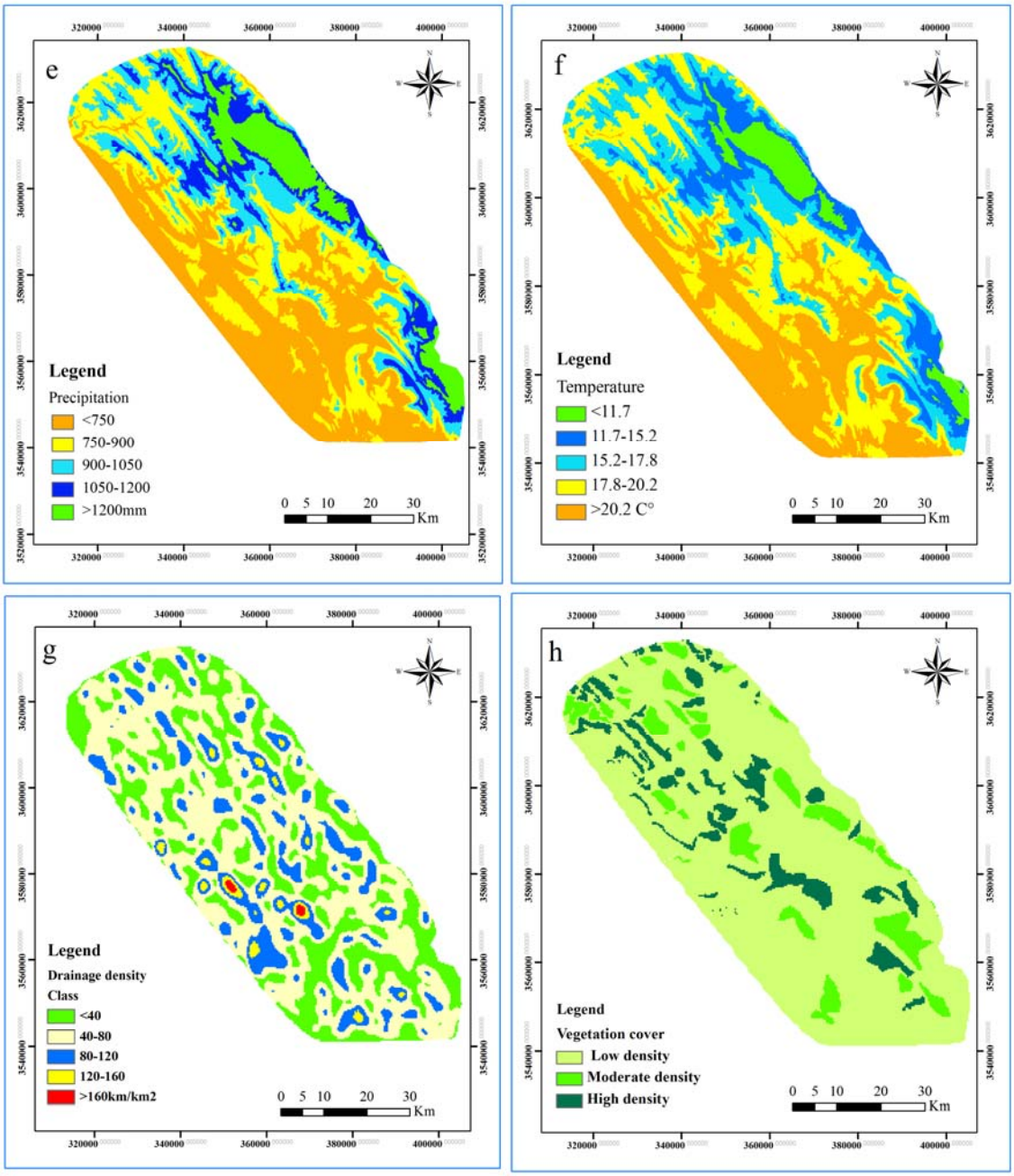

Figure 3. Maps of eight causal factors in karstification potentiality

The Digital Elevation Model (DEM) was created from the available topography maps with scale 1:250,000 from Institute of Geology and Mineral Exploration. The thematic map of elevation was divided into five classes with different ranges: a) <987 m, b) 987- 1459 m, c) 1459-1980 m, d) 1980-2672 m, e) >2672 m (Fig. 3c).

Slope

Slopes were produced after the DEM in Arc Map 9.3. The values (in degrees) were reclassified into classes as shown in table 2. In general, slopes rule the ability of surface water either to remain on the surface long enough to infiltrate or to continue to flow. Usually, the steep slopes indicate greater water velocity. Therefore, it is observed that in the areas of steeper relief, runoff is increased which in turn minimizes the degree of groundwater recharge (Doll *et al.*, 2002). On the contrary, on the relatively gentle sloping terrains, the groundwater

potentiality and karstification potentiality increases due to greater infiltration i.e. the lower the slope, the greater the recharge (Fig. 3d). The slope factor was assigned a weight of 2% (0.02) in the calculation of the karstification potentiality final map, pursuant to AHP method.

Precipitation (rainfall)

This is one of the most important factors and was assigned a weight of 14% (0.14) in the final karstification potentiality value. The higher the precipitation, the higher the karstification potentiality will be. During the present study, monthly rainfall data were collected from 8 stations of the wider area in combination with the Digital Elevation Model (DEM). The mean annual rainfall ranges from 450 to 700 mm in the lowland areas, while in the mountainous areas, rainfall was identified with the altitude. A regression line indicates the following relationship between the rainfall (P in mm) and the altitude (h in m): P = 0.671 h + 314.2. The above relationship was used to illustrate the rainfall map. The resulting map was classified into five major classes (Table 2 and Fig. 3e) : >1200 mm/yr (Very High), 1050– 1200 mm/yr (High), 900–1050 mm/yr (Moderate), 750–900 mm/yr (Low), and <750 mm/yr (Very Low). From the rainfall map, it is observed that in comparison to areas of lower altitude, in areas with higher altitude and rainfall, greater potentiality of karstification exists. About 67–78% of annual rainfall occurs in 5-6 months (October-April next year), while summers are usually dry.

Temperature

Due to the role of temperature in karstification, this data layer was created. The lower the temperature, the higher the karstification potentiality will be. During the present study, monthly temperature data are collected from 8 stations of the wider area in combination with the Digital Elevation Model (DEM). The mean annual temperature ranges from 4.9 to 27 C° in the study area. A regression line indicates the following relationship between the temperature (T in mm) and the altitude (T in C°): T = -0.005h + 25.35. The above relationship is used to illustrate the temperature map. The resulting map is classified into five major classes (Table 2 and Fig. 3f): >20.2 C° (Very Low), 17.8– 20.2 C° (Low), 15.2–17.8 C° (Moderate), 11.7–15.2 C° (High), and <11.7 C° (Very High). This factor is given a weight of 4% (0.04) in this analysis.

Drainage density

Drainage density is the total length of all the streams and rivers in a drainage basin divided by the total area of the drainage basin. It is a measure of how well or how poorly a watershed is drained by stream channels. The drainage network of the study area was created from the DEM through a commands' sequence in ArcMap 9.3 and its density (Fig. 3g) was calculated using the ''Line Density'' command. Next, a reclassification of the raster drainage network density file followed, into 5 classes, from very low to very high, according to the class boundaries of table 2, yielding desired map as shown in Figure 3g. According to geomorphological knowledge, the denser the drainage is, the less the recharge rate will be and vice versa. Hence, in the green-colored areas the karstification potentiality is higher than that in the areas of high drainage density (Fig.3g). The raster drainage network density file was assigned a weight of 3% (0.03) in the calculation of the karstification potentiality final map, based on AHP method.

Vegetation cover

Vegetation cover controls the infiltration of rainwater into subsurface and recharge processes. Vegetation cover is an indicator for the suitability of groundwater prospect. In the high density vegetation area, the surface runoff is slow allowing more time for rainwater to percolate, whereas low density vegetation area facilitate high runoff allowing less residence time for rainwater hence comparatively less infiltration is there (i.e. Infiltration is straightly related to Vegetation cover). In this study, a single date image by Landsat ETM^+ is used to generate land cover types and is assigned a weight of 6% (0.06) in the final karstification potentiality value. The study area is divided into three land cover classes (Table 2). Areas are covered by low density, moderate density and high density vegetation (Fig. 3h).

Final maps

After the procession of all aforementioned factors, the final maps of potentiality of karstification occurrence in the northeast of Khuzestan area were constructed applying two methods. The procedure followed is based on multiplying to the following equation (Elewa & Qaddah, 2011); E being the final karstification potentiality value used in AHP and fuzzy logic methods:

E= 0.38 × Lithology + 0.20 × Lineaments and faults + 0.09 × Elevation + 0.02 × Slope + 0.14 × Rainfall + 0.04 × Temperature +0.03 × Drainage network +0.06 × Cover vegetation (2)

The resulting values were reclassified into five classes with karstification potentiality from very low to very high owing to the grading method of natural break (Fig. 4 & Fig. 6). This is attributed as: non karstic means the area without any karst feature, low means karst topography as found on thin, impure, or chalky limestone where surface drainage and dry valleys are present in addition to some karstic features, moderate means a karst area in which it cannot be seen karst feature such as polje, cave, sinkhole and karst spring with considerable discharge, high and very high means a karst area with little or no surface runoff or streams; it is underlain by thick carbonate rocks and is characterized by well-developed karst surface topography from karren to poljes, extensive subsurface karst features like caves, caverns, galleries, chimneys, etc. According to the final maps produced by AHP and fuzzy logic methods, the area covered by the above classes was calculated and distribution of karstification potentiality classes in the study area shown in Figures 5 and 7. It appears that areas of high and very high potentiality produced by AHP method occupy an area of 1328km^2, while non karstic and low potentiality cover an area of in an area of 1560 km^2. Moderate karstification occurs in an area of 1374 km^2, which covers the largest part of the study area. These amounts about to fuzzy logic method are as follows: 868km^2 (non karstic), 1047 km^2 (low), 1169 km^2 (moderate), 781 km2 (high), and 402 km^2 (very high). The lithological formations with the highest potentiality for karstification are the limestones and dolomites in the study area. The high potentiality for karstification in the limestones is attributed to the high amounts of rainfall, fractures existing and potential recharge, in contrast with the alluvial Formation which are rendered to non karstic potentiality owing to their hydrogeological and morphological characteristics. The karstification potentiality map can be a useful tool in order to identify new supply sources for water. The proposed method is suitable for areas where carbonate rocks are characterized by high degree of karstification. However, the flexibility of this method allows the revision of the weights and rating of parameters in order for other regions to be suitable according to their specific characteristics.

Hydrogeological characteristics

The karst springs in the study area represent natural exits for groundwater. Springs appear at the contact between fractured Asmari limestone rock and low permeability Pabdeh Formation (DA and SH) and in the Asmari Formation itself (AS). The karstic springs can be classified in terms of high to low discharge. The high discharge springs with considerable variation (DA and SH) and low discharge spring with limited variation (AS) reflect the geometrical nature of the karstic systems. Lithological and geological structure studies and the position of the springs (DA, SH and AS) indicate rising up of the springs from three different catchments. The catchment area of DA and the ephemeral SH springs are marked by a density of longitudinal and lateral fractures and these, govern water input and movement. Small fissures and voids feed the AS spring. Probably regolith development is retarding fracture expansion in the spring watershed. Hydrodynamic characteristics perceived at the outlet of major springs consisting of (DA), (AS) and (SH) revealed poorly and well developed karstified systems. The collected data indicated that ponor and polje are operating as underground transporting systems and convey drained water from two smaller reservoirs (AS and SH) into the main reservoir (DA). The same discharge curves are also used to determine flow characteristics and hydrodynamic nature of the karstic system in the area. Based on aforementioned explanation and as shown in Figs. 9a and 9b, hydrographs for DA, SH and AS springs were prepared. It is evident that the flow considerably varies with time for DA and SH springs exhibiting turbulent flow (Fig. 9a) while the AS spring (Fig. 9b) does not depict variation with rainfall. Factors controlling conduit flow of springs include presence of faults (CMF and ShF), highly fractured rocks, and considerable thickness of karstic rocks (250m). In addition, water movement at the floor of poljes plays a significant role such as the DA spring catchment with its remarkable discharge. The catchment area and altitude exit of the springs are given in Table 4. It is evident from Table 4 that catchment area of the DA spring is considerably larger with respect to other springs, and this is influencing outflow discharge of the spring. The turbulent and diffuse flow show development of large fissures to conduits and small fractures to fissures in the catchment areas of DA, SH and AS springs respectively. The discharge curves of springs, which are plotted from daily and

weekly gauge measurement installed at each spring's location, indicate maximum and minimum discharge of the springs. As shown in Figs. 9a and 9b, the discharge of DA and AS springs are sustainable throughout the year, while the SH spring flows only for few months and dries up after rainfall. The same curves have been used for estimation of dynamic potential of springs and as depicted in Table 4, the DA storage potential is appreciable. The Maillet method for defining a hydrograph recession curve in a long-lasting dry period (with no precipitation) and determine springs flow characteristics was used. Eventually, using recession curve analysis and inflection points differentiated conduit flow from base flow.

Calculation of the Catchment Area of springs

The catchment area of each spring was calculated by the following simple water balance equation (Bonacci and Zivaljevic, 1993; Pezeshkpour, 1991; Karimi *et al.,* 2001):

$$A=Q/(P.I)$$

In which A is the catchment area of the spring (km2), Q is the total annual volume of water discharging from the spring [million cubic meters (MCM)], P is the total annual precipitation (m) and I is the recharge coefficient (%).

Determination of recharge coefficient is very difficult. Numerous factors like existence of sinkholes, density of joints and fractures, their openings and type and extent of infillings, percent, thickness and granulation of soil cover, slope of beds and topography, amount, type, time and space distribution of precipitation, temperature, vegetation cover, etc. can affect the recharge coefficient. Recharge coefficient is defined as the percentage of precipitation which contributes to the groundwater storage (spring water). In order to determine the catchment area, it is necessary to have a good approximation of the recharge coefficient for the study area. If there is no idea about the recharge coefficient, the catchment area could be calculated by different recharge coefficients and it will be verified by the proposed method for determining the boundary of a catchment area.

Based on experiences in Zagros Mountain Ranges (Water Resources Investigation and Planning Bureau, 1993; Rahnemaaie, 1994; Raeisi, 1999; Karimi *et al.*, 2001) recharge coefficients can vary between 40 to 90 percent. The lower limit is related to areas of low precipitation, high temperature and evaporation and thick soil coverage. The upper limit represents the existence of sinkholes and well developed karst systems. Based on vegetation, soil coverage, joints and field observations in the ChMA and also previous studies in the Zagros (Pezeshkpour, 1991; Water Resources Investigation and Planning Bureau, 1993; Rahnemaaie, 1994; Karimi *et al.,* 2001), the recharge coefficient is estimated to be 0.5 for the karstic formations of the study area. Using the calculated approximate catchment area, the most probable location and boundaries of the catchments were determined by the following procedure (Karimi, 2003): Step 1: All limestone in the anticline related to the spring and the neighbouring anticlines with higher elevations than the spring will be considered as the catchment area. Step 2: In the area determined in step 1, there must be no hydrogeological and tectonic barriers disconnecting the hydrogeological relationship between the karst aquifer and the spring; In other words, geological and tectonic settings justify the catchment area. Exact and very good geological cross sections could be very useful in this stage. Areas with hydrogeological barriers will be disregarded from the catchment area. Step 3: The general water balance of the area determined in the step 2 will be considered; i.e. all the outputs (including discharge to alluvium) and also all the inputs will be taken into account, so that the catchment area of the spring does not interfere with the other springs. The catchment area is probably as close as possible to the spring, i.e. at first; the catchment

The catchment areas determined with a high uncertainty about them, could be verified using tracing and geophysical tests. Because of the uncertainty in recharge coefficient, the error in the determined catchment area could be as high as 10 percent. Using the above procedure and criteria, the most probable catchment area of the springs are determined.

Analytical Hierarchy Process (AHP)

AHP is a multi-objective, multi-criteria decision-making approach which enables the user to arrive at a scale of preference drawn from a set of alternatives (Ayalew *et al.,* 2005).To apply this approach, it is necessary to break a complex unstructured problem down into its component factors; arrange these factors in a hierarchic order; assign numerical values to subjective judgments on the relative importance of each factor; and synthesize the judgments to determine the priorities

to be assigned to these factors (Saaty & Vargas, 2001). In the construction of a pair-wise comparison matrix, each factor is rated against every other factor by assigning a relative dominant value between 1 and 9 to the intersecting cell (Table. 2). When the factor on the vertical axis is more important than the factor on the horizontal axis, this value varies between 1 and 9. Conversely, the value varies between the reciprocals 1/2 and 1/9 (Table.3). In these techniques, firstly, the effects of each parameter to the occurring karstification relative to each other were determined by dual evaluation in determining the preferences in the effects of the parameters to the karstification potentiality maps. Normally, the determination of the values of the parameters relative to each other is a situation that depends on the choices of the decision-maker. Consequently, the weight values were accurately determined for the real land data (Table 2 & Table 3). In this study, spatial databases were used; the findings were obtained as a result of the field and office studies carried out to create karstification potentiality maps. The analysis of data layers converted to a raster data model was completed by determining their weights in terms of both data layers and sub-criteria, in consequence of the calculation carried out according to the AHP. For all the models, where AHP was used, the CR (Consistency Ratio) was calculated (Saaty, 1977). The models with a CR greater than 0.1were automatically rejected. With the AHP method, the values of spatial factors' weights were defined.

Fuzzy logic

The idea of fuzzy logic is to consider the spatial objects on a map as members of a set (Zadeh, 1965). In classical set theory, an object is a member of a set if it has a membership value of 1, or not a member if it has a membership value of 0. In fuzzy set theory, membership can take on any value between 0 and 1 reflecting the degree of certainty of membership. Fuzzy set theory employs the idea of a membership function that expresses the degree of membership with respect to some attribute of interest. Working in GIS with map layers, generally the attribute of interest is measured over discrete intervals, and the membership function can be expressed as a table relating map classes to membership values. Fuzzy logic is attractive because it is straightforward to understand and implement. It can be used with data from any measurement scale and the weighting of evidence is controlled by the expert.

Fuzzy logic method allows for more flexible combinations of weighted maps, and can be readily implemented with a GIS modeling language.

Table 4. The physical characteristics of the springs

Spring	Type	Altitude (m)	Catchment area (km2)	Discharge (m3)	Dynamic storage (MCM/Annum)
DA	Conduit	550	154	0.7–5	81
SH	Conduit	874	19	0–1.7	10
AS	Diffuse	950	5	0.04–0.05	1.07

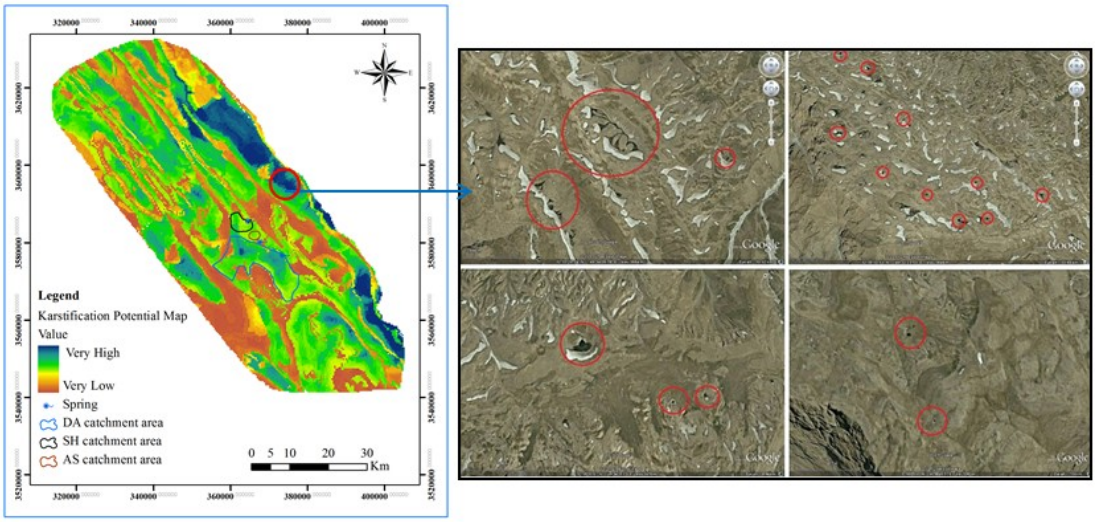

Figure 4. Karstification potential zones produced by AHP method and its validation of the study area

When using fuzzy logic in karstification potential mapping, the spatial objects on a map are considered as members of a set. For example, the spatial objects could be areas on an evidence map (map of causative factors for karstification potential) and the set defined as ‘‘areas suitable to karstification accruing”. A variety of operators can be employed to combine the membership values when two or more maps with fuzzy membership functions for the same set are available. This study uses the fuzzy gamma operator for combining the fuzzy membership functions.

Validation

Validation is the most important process of modeling in that without validation, the models will have no scientific significance (Chung & Fabbri, 2003). Validation of karstification potential map was done with the existence and location of springs and their catchment area, sinkholes and karst aquifers in the study area (Fig. 4 & Fig. 6). For this purpose, the evidences obtained from Google Earth images and aerial photographs of the study area, as well as field surveys were applied.

The main springs and their catchment area and sinkholes detected in this method, overlaid over the final output map of karstification prospect zones and it was found that high to very high karstification potential zones delineated in this research using RS and GIS tools with AHP and Fuzzy logic techniques coincide with sinkhole density (Which are directly responsible for the recharging groundwater area) and also the emergence of springs with considerable discharge rates (from 500 to more than 3000 lit/s), whereas in the regions delineated under moderate to poor karstification potential, no spring or sinkhole was detected.

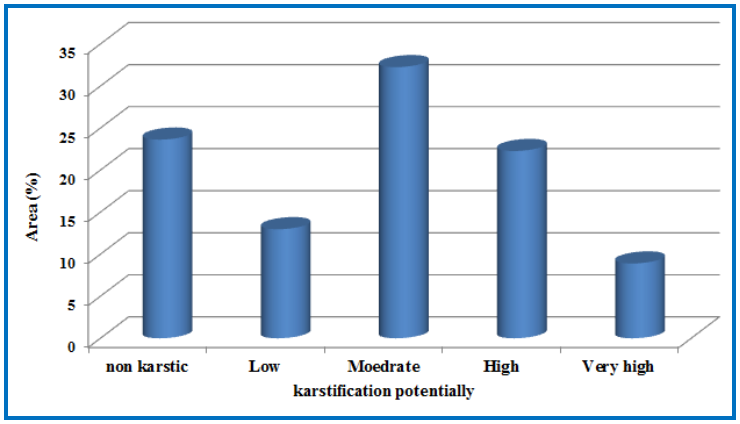

Figure 5. Distribution of karstification potentiality classes in the study area according to AHP methodology

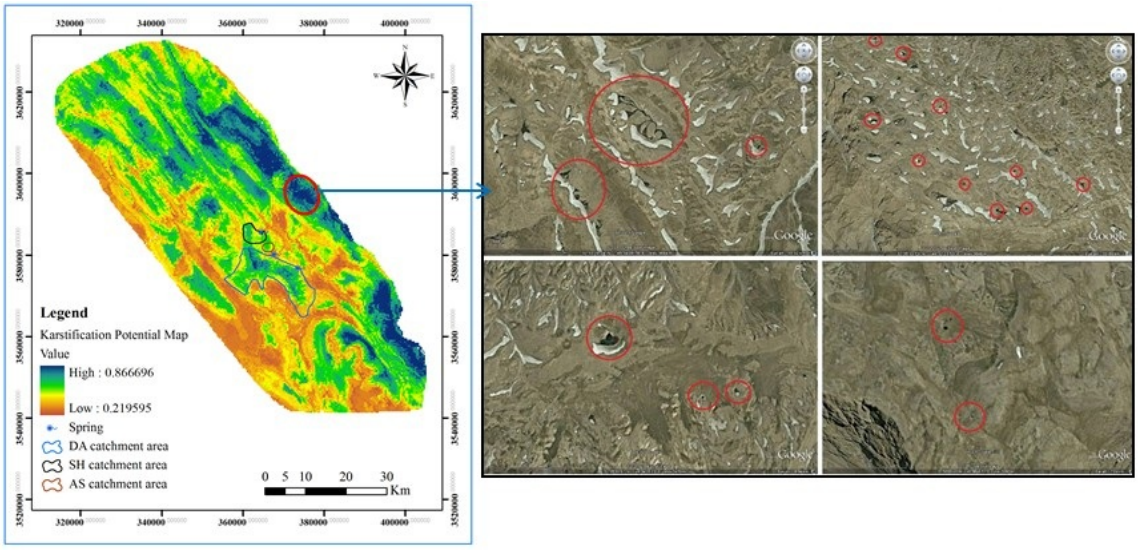

Figure 6. Karstification potential zones produced by Fuzzy logic method and its validation of the study area

Additional uncertainties in mapping the spatial distribution relates to the compatibility between the scale and the resolution of the mapping technique (Tweed *et al.*, 2007). Although the high cost for the water transfer is the main reason for the absence of the borehole, it could be used as a backup water resource region for future use. Thus, the finding of this research establishes the accuracy of the techniques for karstification potential zone mapping and can be used for other regions having similar geological settings. DA, SH and AS are three major springs in the study area that their catchment area located in high and very high karstification potential zones (Fig. 8).

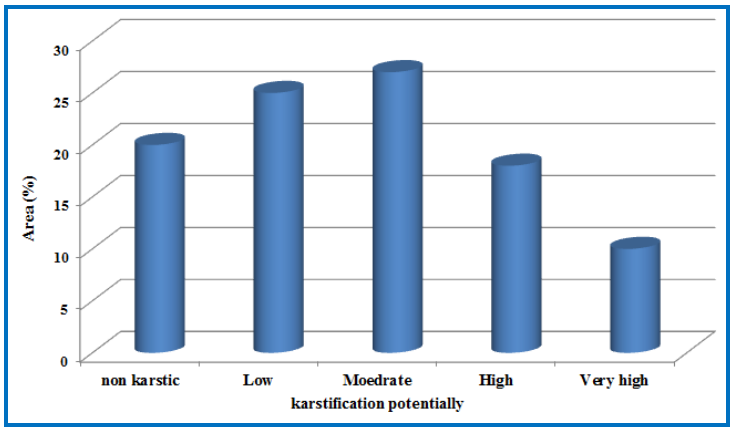

Figure 7. Distribution of karstification potentiality classes in the study area according to Fuzzy logic methodology

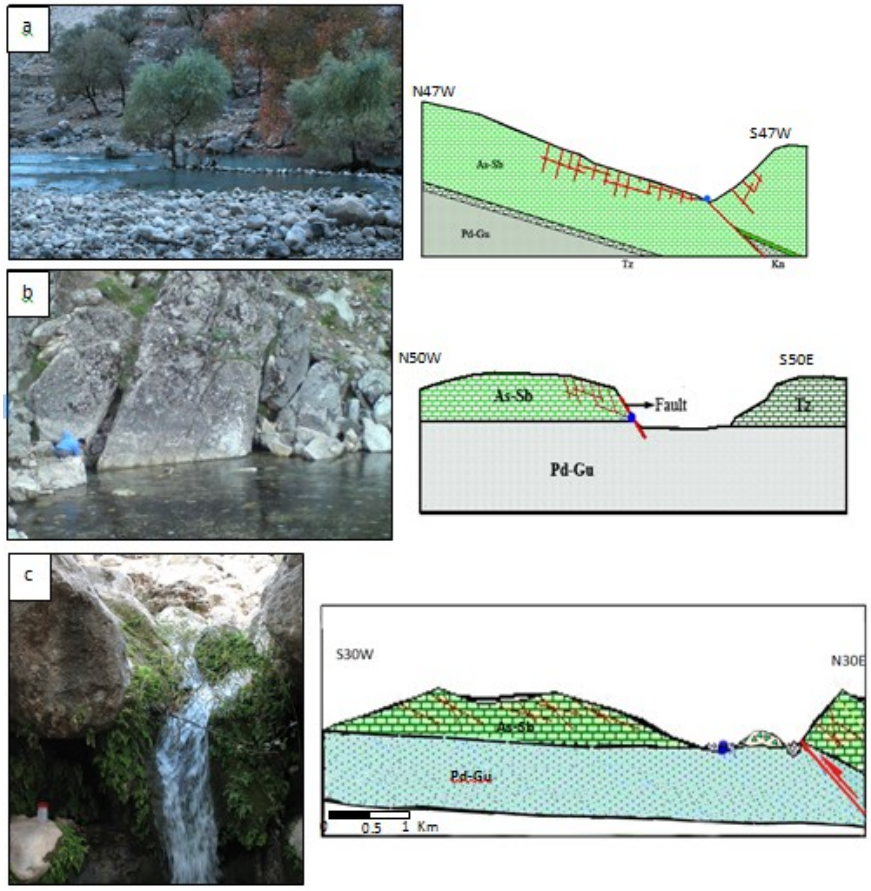

Figure 8. Karst springs and their cross sections in the study area DA (a), SH (b), AS(c)

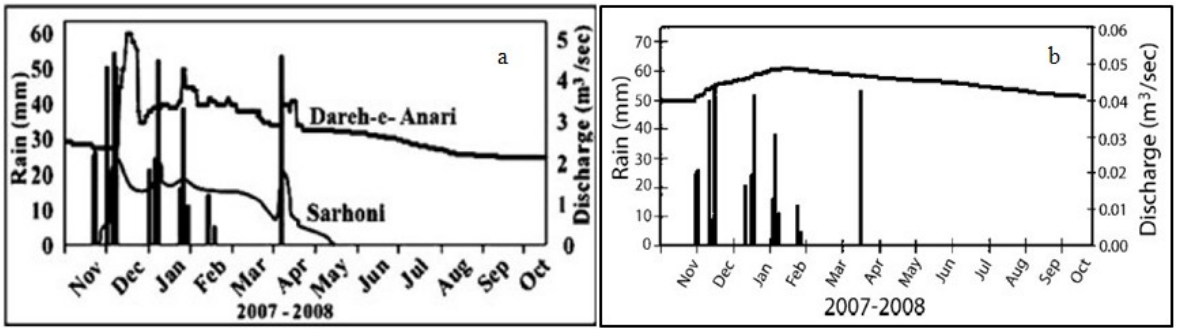

Figure 9. Springs hydrograph a) DA and SH b) AS

Conclusions

One of the main factors for karst development in the area is tectonic activity and occurrence of lineaments in various scales. Structural processes are responsible for the distinct karstic zones and polje development. The hydraulic connection between springs is governed by fault, poljes and ponors. The frequency of longitudinal and lateral fractures trending N30W and N45E respectively in SH and DA catchments are significant for aquifers recharge. These fractures are responsible for quick response of aquifers to events. Due to various sources of recharge and the large catchment area, DA flows throughout the year while SH discharge ends within a short period after rainfall. The fracture development in the AS tract is negligible and its recharge and discharge are strongly related to open spaces and small fissures. This spring flows throughout the year with minor discharge fluctuation.

In this study, both fuzzy logic based approach and analytical hierarchy process (AHP) have been used for identifying the areas prone to karstification potentiality in the wider area of Khuzestan province. Eight parameters with different weights (lithology, lineament density, elevation, slope, rainfall, temperature, drainage density, and vegetation cover) are used that result into two final maps. The limestones and dolomites are the geological formations with the highest potentiality for karstification. The very high to high potential zones are characterized by the higher lineament density, higher rainfall, and lithology type such as limestone and dolomite in most parts of the study area. On the other hand, moderate to poor karstification potential zones are characterized by the lesser lineament density, lower rainfall, lithology type of shale and marl in other parts of the study area. The validity of the illustrated maps is also checked using available data. The validation result shows that the fuzzy logic model has better predication accuracy than the AHP model. Here, the authors conclude that the results of the fuzzy logic model have shown the best prediction accuracy in karstification potentiality mapping in the study area. The maps obtained by these methods can be used by local authorities and water policy makers as a preliminary reference in selecting suitable sites for drilling boreholes. Therefore, the identification of areas, where aquifers are developed can contribute to the rational exploitation and sustainable development of water resources. The flexibility of the methods allows the revision of the weights of included parameters, so the methods can be applied in a wider variety of regions.

References

Abbaspour, KC., Faramarzi, M., Ghasemi, SS., Yang, H., 2009. Assessing the impact of climate change on water resources in Iran. water resources research, 45: 1-16

Aghanabati, A., 2004. Iran's Geology, Publication of Geology Organization (In Persian)

Alavi, M., 2004. Regional stratigraphy of the Zagros Fold-Thrust Belt of Iran and its proforeland evolution. American Journal of Science, 304: 1-20

Antonakos, A., Voudouris, K., Lambrakis, N., 2014. Site selection for drinking-water pumping boreholes using a fuzzy spatial decision support system in the Korinthia prefecture, SE Greece. Journal of Hydrogeolgy, 22: 1763-1776.

Ashjari, J and Raeisi, E., 2006. Influences of anticlinal structure on regional flow, Zagros, Iran. Journal of Cave and Karst Studies, 68(3): 118-129.

Ayalew, L., Yamagishi, H., 2005. The application of GIS-based logistic regression for landslide susceptibility mapping in the Kakuda–Yahiko Mountains, Central Japan. Geomorphology, 65: 15-31

Ayazi, MH., Pirasteh, S., Arvin, AKP., Pradhan, B., Nikouravan, B., Mansor, S., 2010. Disasters and risk reduction in groundwater: Zagros Mountain Southwest Iran using geo-informatics techniques. Dis Adv, 3(1): 51-57

Baghvand, A., Nasrabadi, T., Bidhendi, GN., Vosoogh, A., Karbassi, A., Mehrdadi, N., 2010. Groundwater quality degradation of an aquifer in Iran central desert. Desalination, 260: 264–275.

Banai-Kashani, R., 1989. A new method for site suitability analysis: The analytic hierarchy process. Env. Manage, 13: 685-693.

Bastani, M., Kholghi, M., Rakhshandehroo, GR., 2010. Inverse modeling of variable-density groundwater flow in a semi-arid area in Iran using a genetic algorithm. Journal of Hydrogeology, 18: 1191-1203

Black, T.J., 1997. Evaporite karst of northern lower Michigan. Carbonates and Evaporites, 12: 81-83.

Bonacci, O., Gottstein, S., Roje-Bonacci, T., 2009a. Negative impacts of grouting on the underground karst environment. Ecohydrology, 2:492-502.

Bonacci, O., Pipan, T., Culver, D.C., 2009b. A framework for karst ecohydrology. Environmental Geology, 56: 891-900.

Bonacci, O., Roje-Bonacci, T., 2008. Water losses from the Ricice reservoir built in the Dinaric karst. Engineering Geology, 99:121-127.

Calaforra, J.M., Pulido-Bosch, A., 2003. Evolution of the gypsum karst of Sorbas (SE Spain). Geomorphology, 50:173–180.

Chitsazan M., Karimi Vardanjani H., Karimi H., Charchi, A., 2015. A comparison between karst development in two main zones of Iran: case study-Keyno anticline (Zagros Range) and Shotori anticline (Central Iran). ArabJ Geosci. doi:10.1007/s12517-015-1961-x

Chung, C.J.F., Fabbri, A.G., 2003. Validation of spatial prediction models for landslide hazard mapping. Nat Hazards, 30(3): 451-472

Cvijic, J., 1893. Das Karstphänomen. Versuch einer morphologischen Monographie. Geographische Abhandlungen Wien, 5: 218–329.

De Waele, J., Plan, L., Audra, P., 2009. Recent developments in surface and subsurface karst geomorphology: an introduction. Geomorphology, 106: 1-8.

Doll, P., Lehner, B., Kaspar, F., 2002. Global Modeling of groundwater recharge. In: Proceedings of 3rd International Conference on water resources and the environment research, vol. 1, Technical University of Dresden, Germany, pp. 27-33.

Domakinis, C., Oikonomidis, D., Astaras, T., 2008. Landslide mapping in the coastal area between the Strymonic Gulf and Kavala (Macedonia, Greece) with the aid of remote sensing and Geographical Information Systems. Intern. J. Rem. Sens, 29 (23): 6893-6915.

Entekhabi, D., Moghaddam, M., 2007. Mapping recharge from space: roadmap to meeting the grand challenge. Journal of Hydrogeology, 15: 105-116.

Field, M.S., 2010. Simulating drainage from a flooded sinkhole. Acta Carsologica, 39: 361-378.

Ford, D., 2007. Jovan Cvijic and the founding of karst geomorphology. Environmental Geology, 51:675-684.

Ford, D., Williams, P., 2007. Karst hydrogeology and Geomorphology. John Wiley & Sons, New York, Toronto.

Ghayoumian, J., Mohseni Saravi, M., Feiznia, S., Nourib, B., Malekian, A., 2007. Application of GIS techniques to determine areas most suitable for artificial groundwater recharge in a coastal aquifer in southern Iran. Journal of Asian Earth Sci, 30:364-37.

Goldscheider, N., Madl-Szonyi, J., Eross, A., Schill, E., 2010. Review: thermal water resources in carbonate rock aquifers. Journal of Hydrogeology, 18:1303-1318.

Groves, C., Meiman, J., 2005. Weathering, geomorphic work, and karst landscape evolution in the Cave City groundwater basin, Mammoth Cave, Kentucky. Geomorphology, 67: 115–126.

Haririan, M., 1990. Iran's Geomorphology, Publication of Islamic Azad University, pp: 96. (In Persian)

Hosseini, M., Ghafouri, A.M., Amin. M.S.M., Tabatabaei, M.R., Goodarzi, M., Abde Kolahchi, A., 2012. Effects of land use changes onwater balance in Taleghan Catchment, Iran. Journal of Agric Sci Tech, 14:1159-1172.

Huan, H., Jinsheng, W., Yanguo, T., 2012. Assessment and validation of groundwater vulnerability to nitrate based on a modified DRASTIC model: a case study in Jilin City of northeast China. Journal of Sci. Total Environ, 440: 14-23.

Humphreys, W.F., 2006. Aquifers: the ultimate groundwater-dependent ecosystems. Australian Journal of Botany, 54:115-132.

Institute of Geological and Mineral Exploration 1967. Geological maps, sheets: Lali, Keyno and Kamestan. Scale 1:100.000

James, G.A., Wynd, J.G., 1965. Stratigraphic nomenclature of Iranian oil consortium agreement area. American Association of petroleum Geologists Bul, 49: 2182-224

Johnson, S.B., Stieglitz, R.D., 1990. Karst features of a glaciated dolomite peninsula, Door County, Wisconsin. Geomorphology, 4:37-54.

Kalantari, N., Ghafari, H.R., Keshavarzi, M.R., Mallaei, M.R., 2011. Factors impacting on flow pattern in the Shimbar

karstic area in the southwest of Iran. 9th conference on limestone hydrogeology, 2011, Besancon, France.
Karimi, H., Raeisi, E., Zare, M., 2003. Hydrodynamic Behavior of the Gilan Karst Spring, West of the Zagros, Iran. Journal of Cave and Karst Science, 30 (1): 15-22.
Karimi, H., Raeisi, E., Zare, M., 2001. Determination of catchment area of aquifer bearing Tangab dam site using water balance method. Proceedings of The second national conference on engineering geology and the environment, Tehran, 16-18 Oct. 2001, V.2, P. 773-755.
Kazakis, N., Voudouris, K.S., 2015. Groundwater vulnerability and pollution risk assessment of porous aquifers to nitrate: Modifying the DRASTIC method using quantitative parameters. Journal of Hydrolgy, 525: 13-25.
Konkul, J., Rojborwornwittaya, W., Chotpantarat, S., 2014. Hydrogeologic characteristics and groundwater potentiality mapping using potential surface analysis in the Huay Sai area, Phetchaburi Province, Thailand. Journal of Geosci, 18 (1): 89-103.
Leblanc, M., Favreau, G., Tweed, S., Leduc, C., Razack, M., Mofor, L., 2007. Remote sensing for groundwater modelling in large semiarid areas: Lake Cad Basin, Africa. Journal of Hydrogeology, 15: 97-100.
Maleki, D., Shoohani, M., Alaeitaleghani 2009. Zooning of Karst development in Kermanshah provine, Modarres seasonal of humanities, 13th course 1: 272-295 (In Persian)
Moghimi, H., 2010. Karst Hydrology, Publication of Payam-e Noor (In Persian)
Neshat, A., Pradhan, B., Pirasteh, S., Shafri, H.Z.M., 2013. Estimating groundwater vulnerability to pollution using modified DRASTIC model in the Kerman agricultural area. Iran Environ Earth Sci.
Nosrati, K., Eeckhaut, M.V.D., 2012. Assessment of groundwater quality using multivariate statistical techniques in Hashtgerd Plain, Iran. Environ Earth Sci, 65:331-344.
Pezeshkpour, P., 1991. Hydrogeological and hydrochemical evaluation of Kuh-e Gar-Barm-Firooz springs, Unpublished M.Sc. Thesis, Shiraz University, pp. 282.
Pourghasemi, H.R., Pradhan, B., Gokceoglu, C., 2012. Application of fuzzy logic and analytical hierarchy process (AHP) to landslide susceptibility mapping at Haraz watershed, Iran. Nat. Hazards, 63: 965-996.
Raeisi, E., 1999. Calculation method of karst water balance in Zagros Simple Folded zone, Proceedings of the first Regional Conference on water balance, Ahwaz, p. 39-49.
Rahmati, O., 2013. An investigation of quantitative zonation and groundwater potential (case study: Ghorveh-Dehgolan plain). M.Sc. thesis, Tehran University.
Rahnemaaie, M., 1994. Evaluation of infiltration and runoff in the karstified carbonatic rocks, Unpublished Master of Science Thesis, Shiraz University, Iran.
Ravbar, N., Goldscheider, N., 2007. Proposed methodology of vulnerability and contamination risk mapping for the protection of karst aquifers in Slovenia. Acta Carsologica ,36: 397-411.
Saaty, T.L., 1980.The Analytic Hierarchy Process. McGraw Hill, New York.
Saaty, T.L., 1977. A scaling method for priorities in hierarchical structures. Journal of Mathematical Psychology, 15: 234-281.
Saaty, T.L., Vargas, G.L., 2001. Models, Methods, Concepts, and Applications of the Analytic Hierarchy Process. Kluwer Academic Publisher, Boston.
Stocklin, J., Setudehnia, A., 1977. Stratigraphic lexicon of Iran. Geology Survey of Iran, 376 pp
Tweed, S.O., Leblanc, M., Webb, J.A., Lubczynski, M.W., 2007. Remote sensing and GIS for mapping groundwater recharge and discharge areas in salinity prone catchments, SE Australia. Journal of Hydrogeology, 15: 75-96.
Vigna, B., Fiorucci, A., Banzato, C., Forti, P., De Waele, J., 2010. Hypogene gypsum karst and sinkhole formation at Moncalvo (Asti, Italy). Zeitschrift für Geomorphologie, 54, 285–306.
Fu Yeh, H., Sin Cheng, Y., I. Lin, H., Haw Lee, Ch., 2016. Mapping groundwater recharge potential zone using a GIS approach in Hualian River, Taiwan, Sustainable Environment Research journal, in press.
Water Resources Investigation and Planning Bureau 1993. Comprehensive study and research in water resources of the Maharlu karst basin (Fars). Vol.1-4.
Zadeh, L. A., 1965. Fuzzy sets. Information and Control, 8:338-353.
Zarghami, M., Abdi, A., Babaeian, I., Hassanzade, Y., Kanani, R., 2011. Impacts of climate change on runoffs in East Azerbaijan, Iran. Glob Planet Chang, 78(3-4):137-146.